

Tom Y. Otoshi

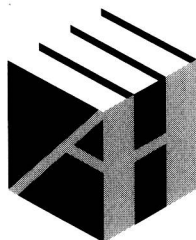
**NOISE
TEMPERATURE
THEORY AND
APPLICATIONS
FOR DEEP SPACE
COMMUNICATIONS
ANTENNA SYSTEMS**



TN822
088

Noise Temperature Theory and Applications for Deep Space Communications Antenna Systems

Tom Y. Otoshi



**ARTECH
HOUSE**

BOSTON | LONDON
artechhouse.com

Library of Congress Cataloging-in-Publication Data

A catalog record for this book is available from the U.S. Library of Congress.

British Library Cataloguing in Publication Data

A catalogue record for this book is available from the British Library.

ISBN-13: 978-1-59693-377-4

Cover design by Igor Valdman

© 2008 ARTECH HOUSE, INC.

685 Canton Street

Norwood, MA 02062

All rights reserved. Printed and bound in the United States of America. No part of this book may be reproduced or utilized in any form or by any means, electronic or mechanical, including photocopying, recording, or by any information storage and retrieval system, without permission in writing from the publisher.

All terms mentioned in this book that are known to be trademarks or service marks have been appropriately capitalized. Artech House cannot attest to the accuracy of this information. Use of a term in this book should not be regarded as affecting the validity of any trademark or service mark.

10 9 8 7 6 5 4 3 2 1



Noise Temperature Theory and Applications for Deep Space Communications Antenna Systems

as in the Attach
turn to the back

*To my wife Haruko Shirley Otoshi, my son John Terence Otoshi, and my daughter
Kathryn Ann Otoshi, who all shared in my 40 or more years of aspirations and
endeavors at the Jet Propulsion Laboratory, California Institute of Technology in
Pasadena, California*

Foreword

Of the many technical considerations that go into realization of the large NASA-JPL ground antennas of the Deep Space Network (recently redesignated the Inter-Planetary Network), it is the critical microwave receive system performance that often limits deep-space mission data return. Receive system performance is governed by the ratio of gain to noise temperature (G/T), with gain (proportional to the antenna effective collecting area) providing the received signal level; T refers to the underlying noise level or noise temperature, a bandwidth-independent noise power measure. Perhaps obvious, it is vital to maximize G , while minimizing T in such high-performance receive systems.

Author Tom Y. Otoshi spent the major part of his more than 40-year career at JPL analyzing, designing, and accurately evaluating many of the detailed elements that comprise minimizing, then stating with known error confidence, the receive system noise temperature. Otoshi remains one of those rare individuals with a commanding presence in both theoretical and practical microwave matters and metrology, as can be seen in his impressive bibliography.

In this volume the author first provides the introductory topics necessary and convenient for reader overview. The author then discusses a variety of reflector performance issues, including important detailed information on material conductivities, perforations, protective coatings, terrestrial weather effects, and the influence of the Earth's Sun.

Throughout, the author provides highly useful information for microwave engineers in many allied disciplines, including measurement and accuracy evaluation strategies. In Chapters 4–6 the author continues with error analyses, tutorials and in our considered opinion, a collection of highly useful formulae perhaps never before collected in one compact document. Of especial note in Chapter 5, the author presents for the first time known to us, a practical method for noise temperature prediction of multiports, by use of S -parameters.

Practicing microwave engineers in many related fields will likely refer to this carefully considered book, thereby earning it a convenient and permanent place on their bookshelves.

Dan A. Bathker (JPL, Ret.)

Stephen D. Slobin, JPL

May 2008

Preface

The importance of minimizing noise temperatures in antenna systems has been stated in the Foreword by Bathker and Slobin and will not be restated here. The author assumes that the reader is somewhat familiar with the fundamentals of noise temperature and knows that a basic antenna receiving system consists of an antenna, the interconnecting network, the front-end low-noise amplifier, and the follow-up receiver. The book starts by discussing the theory of antenna noise temperature for a simple antenna, such as a horn or parabolic antenna, and how to calculate noise contributions from the cosmic background, the galaxy (negligibly small above 8 GHz), the atmosphere, ground, reflector spillover, and reflector surface losses. The noise temperature of a beam waveguide antenna system is described as well as the noise temperature of a dichroic plate installed in the system. Subsequent chapters discuss the noise generated by microwave networks between the receive horn and the front-end low-noise amplifier. This book does not cover the theory of noise generated by the front-end low-noise amplifier or the follow-up receiver. For this information, the reader can refer to books on these subjects.

This book aims to present selected topics related to noise temperature measurements and analyses that the author has performed on deep space antennas and microwave systems in the NASA/JPL Deep Space Network (DSN). Some materials have been extracted from JPL or IEEE Publications while other materials in Section 1.1 and Chapter 5 are new and have not been previously published.

Highlights of the chapters in this book are described as follows: Chapter 1 covers introductory topics, including calculating antenna noise temperature as a function of pointing angles from the sky at zenith to the horizon accounting for ground absorption and reflection. Chapter 1 also describes two methods of extracting atmospheric noise temperature at zenith from tipping curve measurements. In addition, Chapter 1 discusses a unique method that was used for evaluating the performance of a new beam waveguide antenna system through the use of portable test packages used to make measurements of system noise temperature and gain at three of the beam waveguide antenna focal points. Chapter 2 provides the theoretical and measured noise temperatures of reflector surfaces including solid-, perforated-, painted- and wet-panels. Chapter 3 covers noise temperature experiments, including: (1) the effects of different gain horns at the Cassegrain focal point on antenna noise temperature, (2) the design of a transparent net placed over the beam waveguide antenna opening to keep birds out, (3) various experiments to lower the system noise temperature, and (4) an absorber sheet method to measure the Sun's noise temperature (10,000K) without saturating the receiver. Chapter 4 describes some fundamentals of noise temperature and mismatch

theory as applied to basic receive systems. Chapter 4 also presents tables of mismatch error equations in terms of both reflection coefficient magnitudes and VSWRs useful for determining the effects of mismatch on the calibration of system noise temperature and antenna efficiency. In addition, Chapter 4 details equations for determining the equivalent source temperature of cascaded mismatched networks as well as the equivalent input noise temperature of cascaded mismatched networks. Chapter 5 provides a network analysis method for determining the noise temperature of a multiport having two internal paths from source port to the output port and in addition considers the case of two external noise sources connected to a multiport. The author believes that an easy to understand presentation has been offered for a methodology of using S-parameters to analyze noise generated by multiport networks. All the material in Chapter 5 was previously published in an internal JPL report in September 2004, but it was not available to engineers outside of JPL. Finally, Chapter 6 provides useful and simple formulas for calculating the noise temperatures of a solid metallic reflector surface, perforated plates, and wire grids as functions of frequency, incidence angle, and polarization.

The author believes that this is the first book on noise temperature intended for the practicing engineer in the field of developing low-noise large microwave antennas for deep-space communication. The author hopes that the material in this book is a good mix of background theory and practical examples that will allow the reader to learn in a short time what the author learned over 43 years at JPL: a comprehensive understanding of the noise generated by the antenna and the environment and microwave networks and receivers following the feed. Mismatch error analyses are a subject generally avoided. This book, however, presents a table of useful mismatch error equations in terms of both reflection coefficient magnitudes and VSWRs.

The extensive list of personnel who contributed in various ways to make this book possible are recognized in the Acknowledgments.

The author takes sole responsibility for the accuracy of any new material that has not been previously published in JPL Progress Report or IEEE articles.

Acknowledgments

The author would like to specially acknowledge Stephen D. Slobin (JPL) and Dan A. Bathker (JPL-Ret.) whose behind-the-scene efforts and encouragement made it possible for the material presented in this book to become available to the technical world outside of JPL.

The author also acknowledges the earlier editorial assistance of Pat Ehlers of the JPL Documentation Section on Progress Report articles from which a large portion of material in this book was used. In addition, the author is deeply indebted to Cindy Copeland, who typed the manuscript, created the graphics for this book, and provided invaluable assistance whenever needed. Numerous persons contributed in various ways to the technical work described in this book. Contributors who were sometimes coauthors on progress report articles are listed as follows:

- Section 1.1 and 1.2: Charles Stelzried;
- Section 1.3: Dan Bathker, Scott Stewart, and Manuel Franco;
- Section 1.4: Manuel Franco;
- Section 2.1: Watt Veruttipong;
- Section 2.2: Cavour Yeh;
- Section 2.3: Yahya Rahmat-Samii, Rick Cirillo, Jr., and John Sosnowski;
- Section 2.4: Manuel Franco;
- Section 3.1: Manuel Franco and Paula Brown;
- Section 3.2: Watt Veruttipong and John Sosnowski;
- Section 3.3: Watt Veruttipong, John Sosnowski, and Rick Cirillo, Jr.;
- Section 3.4: Paul Richter, Stephen Keihm, and Stephen Slobin;
- Section 4.1: Charles Stelzried.

The author also gratefully acknowledges the DSS 13 crew of G. Bury (supervisor), J. Garnica, B. Reese, and L. Smith for helping him to perform noise measurements on the large beam waveguide antenna in a challenging field environment. The measurements included test package test evaluations, G/T improvement tests, and difficult Sun experiments. D. Wolff of the Planning Research Corporation (PRC) in Pasadena, California, provided the aluminum dots, and N. Bucknam, formerly of PRC, designed the tapered cone transition used in the G/T improvement tests. The author would also like to give special acknowledgment to J. Garnica who prepared many of the experimental setups at DSS 13 station in advance, so

that the author could perform the tests described in this book efficiently and successfully.

The research described in this publication was carried out at the Jet Propulsion Laboratory, California Institute of Technology, under a contract with the National Aeronautics and Space Administration.

Contents

Foreword	<i>xi</i>
Preface	<i>xiii</i>
Acknowledgments	<i>xv</i>
CHAPTER 1	
Introductory Topics	1
1.1 Antenna Noise Temperature as Functions of Pointing Angles	1
1.1.1 Zenith Formula	1
1.1.2 Sky Brightness Temperature	6
1.1.3 Ground Brightness Temperature	11
1.1.4 Formula for Nonzenith Pointing Angles	17
1.1.5 Tipping Curve Applications	22
1.2 Cosmic Background Noise Temperature	37
1.2.1 Introduction	37
1.2.2 Calibration Equation	37
1.2.3 Experimental Results	39
1.2.4 Commentary	39
1.3 Portable Microwave Test Packages	40
1.3.1 Introduction	40
1.3.2 Test-Package Descriptions	41
1.3.3 Test Configurations and Test Procedure	42
1.3.4 Noise-Temperature Measurement Method	44
1.3.5 Noise-Temperature Measurement Results	47
1.3.6 Concluding Remarks	50
1.4 Dichroic Plate in a Beam-Waveguide Antenna System	50
1.4.1 Introduction	50
1.4.2 Background	51
1.4.3 Analytical Method	54
1.4.4 Experimental Work	62
1.4.5 Conclusions	66
References	66
Selected Bibliography	69

CHAPTER 2

Reflector Surfaces	71
2.1 Perforated Panels	71
2.1.1 Introduction	71
2.1.2 Old Calculation Method	73
2.1.3 New Calculation Method	74
2.1.4 Perforated-Plate and Perforated-Panel Geometries	80
2.1.5 Results	82
2.1.6 Concluding Remarks	86
2.2 Solid Panels	88
2.2.1 Basic Noise Temperature Relationships	88
2.2.2 Dependence on Polarization and Incidence Angle	93
2.2.3 Electrical Conductivity of Various Metals	99
2.3 Painted Panels	108
2.3.1 Background on Paint Study	108
2.3.2 Background on DSN Antennas	108
2.3.3 Excess Noise Temperature and Added Gain Loss	110
2.3.4 Results and Performance Characterizations	113
2.3.5 Conclusions	130
2.4 Wet Panels	131
2.4.1 Theoretical Studies	131
2.4.2 Experimental Studies	132
References	134

CHAPTER 3

Noise Temperature Experiments	137
3.1 Horns of Different Gains at f_1	137
3.1.1 Introduction	137
3.1.2 Analytical Procedure and Results	137
3.1.3 Experimental Work	144
3.1.4 Determination of Strut Contribution	147
3.1.5 Conclusions	151
3.2 Bird Net Cover for BWG Antennas	152
3.2.1 Introduction	152
3.2.2 Description of the Net Cover	152
3.2.3 Test Results	153
3.2.4 Concluding Remarks	155
3.3 G/T Improvement Task	156
3.3.1 Introduction	156
3.3.2 Test Configurations and Test Results	157
3.3.3 Summary and Recommendations	171
3.4 Measured Sun Noise Temperature at 32 GHz	172
3.4.1 Introduction	172
3.4.2 Gain Reduction Methods	173

3.4.3	Measurement and Data Reduction Method	177
3.4.4	Experimental Results	180
3.4.5	Concluding Remarks	185
	References	186
	Selected Bibliography	187

CHAPTER 4

	Mismatch Error Analyses	189
4.1	Antenna System Noise Temperature Calibration Mismatch Errors	189
4.1.1	Introduction	189
4.1.2	Review	190
4.1.3	Antenna System Noise Temperature Measurements	196
4.1.4	Antenna Efficiency Measurements	205
4.1.5	Applications	210
4.1.6	Concluding Remarks	221
4.2	Equivalent Source Noise Temperature at Output of Cascaded Lossy Networks	222
4.2.1	Matched Case	222
4.2.2	Mismatched Case	224
4.3	Effective Input Noise Temperature at Input of Cascaded Lossy Networks	229
4.3.1	Matched Case	229
4.3.2	General Mismatched Case	231
	References	233

CHAPTER 5

	Network Analysis Topics	235
5.1	Two-Port Network Containing Two Internal Paths	235
5.1.1	Introduction and Background	235
5.1.2	Dissipative Power Ratios of Four-, Three-, and Two-Port Networks	235
5.1.3	Power Flow (PF) Method	239
5.1.4	Voltage Wave (VW) Method	242
5.1.5	Sample Cases	246
5.1.6	Example of the Effects of a Mismatched Component in Path 1	249
5.1.7	Conclusions	252
5.2	Three-Port Network with Two External Noise Sources	252
5.2.1	Introduction	252
5.2.2	Properties of an Ideal Four-Port Coupler	253
5.2.3	Two External Noise Source Outputs Travel Common Paths	254
5.2.4	Two External Noise Source Outputs Travel Individual Paths	262
5.2.5	Conclusions	265
	References	266

CHAPTER 6

Useful Formulas for Noise Temperature Applications	269
6.1 Formulas Associated with Solid Metal Reflectors	269
6.1.1 Conductivity of Metals	269
6.1.2 Noise Temperature of a Solid Metallic Sheet	270
6.2 Formulas Associated with Metal Reflectors with Holes	271
6.2.1 Perforated Plates with Round Holes	271
6.2.2 Wire Grids	274
6.3 Other Useful Formulas	276
6.3.1 Relationship of Insertion Loss to Noise Temperature	276
6.3.2 Relationship of Return Loss to Reflection Coefficient and VSWR	278
References	279
About the Author	281
Index	283

Introductory Topics

1.1 Antenna Noise Temperature as Functions of Pointing Angles

1.1.1 Zenith Formula

For the spherical coordinate system shown in Figure 1.1, the antenna noise temperature equation that accounts for cross-polarization is given in [1] as

$$T_A = \frac{\int_0^{2\pi} \int_0^{\pi} [P_c(\theta, \phi) T_{bc}(\theta, \phi) + P_x(\theta, \phi) T_{bx}(\theta, \phi)] \sin \theta \, d\theta \, d\phi}{\int_0^{2\pi} \int_0^{\pi} [P_c(\theta, \phi) + P_x(\theta, \phi)] \sin \theta \, d\theta \, d\phi} \quad (1.1)$$

where $P_c(\theta, \phi)$ and $P_x(\theta, \phi)$, respectively, are the power per unit solid angles for the copolarized and cross-polarized fields. The symbols T_{bc} and T_{bx} are the brightness temperatures for the copolarized and cross-polarized directions, respectively. Although T_{bc} and T_{bx} are generally the same for the sky region, they are not necessarily the same for the ground region because of ground reflection coefficient dependence on polarization.

If the cross-polarized fields are small relative to the copolarized fields, the equation reduces to the familiar equation,

$$T_A = \frac{\int_0^{\pi} \int_0^{2\pi} P(\theta, \phi) T_b(\theta, \phi) \sin \theta \, d\phi \, d\theta}{\int_0^{\pi} \int_0^{2\pi} P(\theta, \phi) \sin \theta \, d\phi \, d\theta} \quad (1.2)$$

where

$P(\theta, \phi)$ = power per unit solid angle for the copolarized fields in the θ, ϕ direction.

$T_b(\theta, \phi)$ = brightness temperature for the copolarized fields, K.

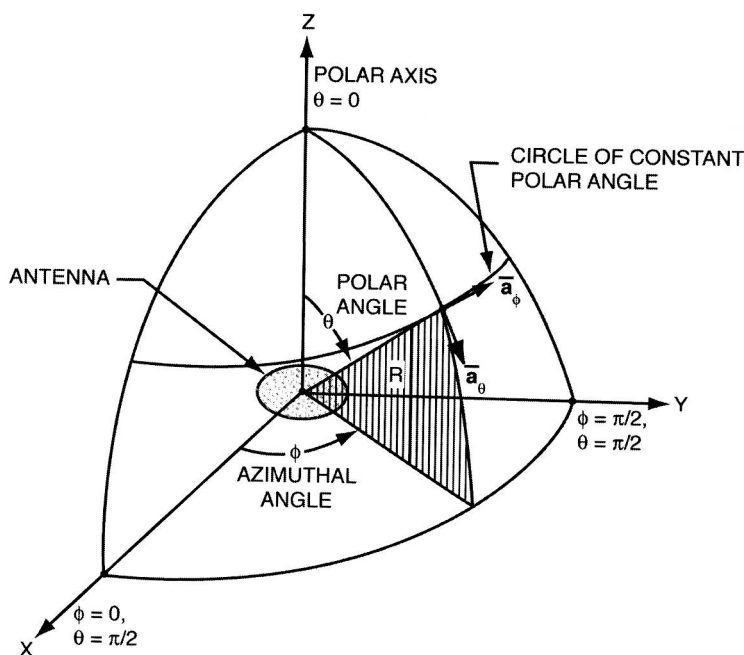


Figure 1.1 The (R, θ, ϕ) spherical coordinate system.

Since the denominator of (1.2) is the total radiated power P_T , and the antenna gain $G(\theta, \phi)$ in any direction is [2]

$$G(\theta, \phi) = 4\pi \frac{P(\theta, \phi)}{P_T} \quad (1.3)$$

substitution into (1.2) gives another familiar expression of

$$T_A = \frac{1}{4\pi} \int_0^\pi \int_0^{2\pi} G(\theta, \phi) T_b(\theta, \phi) \sin \theta d\phi d\theta \quad (1.4)$$

Ludwig [3] pointed out that the total power pattern of an antenna or horn with complete physical circular symmetry can be described in terms of two selected patterns. For a linearly polarized antenna, the two required patterns are the E- and H-plane patterns. For an RCP antenna, the two required patterns are the receive patterns taken with the illuminator, illuminating first in RCP and then in LCP. For an LCP antenna, the two required patterns are LCP and RCP.

The following discussion presents a derivation of the equations for antenna noise temperature of a linearly polarized and circularly symmetric antenna in terms of E- and H-plane patterns. The case for a circularly polarized antenna is not analyzed here, but by expanding the analysis to take into account the 90-degree phase difference between E- and H-plane patterns for the CP case, the derivation to follow can be used for an RCP or LCP antenna.

Following the analysis given by Ludwig in [3], let $\mathbf{E}_0(R, \phi, \theta)$ represent the far-field electric field pattern of any antenna located at the origin of the spherical coordinate system (R, ϕ, θ) , as shown in Figure 1.1. R is defined as the distance of \mathbf{E}_0 from the origin; ϕ is the azimuthal angle in radians; θ is the polar angle in radians; and $\mathbf{a}_R, \mathbf{a}_\phi, \mathbf{a}_\theta$ are the associated unit vectors.

For this analysis, assume that the antenna has complete physical circular symmetry and is excited by the dominant or any $m = 1$ cylindrical mode. The modes of a cylindrical waveguide are given in terms of TE_{mn} and TM_{mn} . For a more general expression of the far-field expansion, refer to discussions on spherical wave functions given by Ludwig in [4, 5]. Then

$$\mathbf{E}_0(R, \phi, \theta) = \frac{e^{-j\kappa R}}{R} [A_1(\theta) \sin \phi \mathbf{a}_\theta + B_1(\theta) \cos \phi \mathbf{a}_\phi] \quad (1.5)$$

where

$$\begin{aligned} \kappa &= \frac{2\pi}{\lambda} \\ A_1(\theta) &= |A_1(\theta)| e^{j\Phi_{A_1}(\theta)} \\ B_1(\theta) &= |B_1(\theta)| e^{j\Phi_{B_1}(\theta)} \end{aligned}$$

The subscript 1 is used to identify the $m = 1$ cylindrical mode. The terms $|A_1(\theta)|$, $|B_1(\theta)|$, $\Phi_{A_1}(\theta)$, and $\Phi_{B_1}(\theta)$ will be defined in the following: Note that if $\phi = 0$, (1.5) becomes

$$\mathbf{E}_0(R, 0, \theta) = \frac{|B_1(\theta)|}{R} e^{-j[\kappa R - \Phi_{B_1}(\theta)]} \mathbf{a}_\phi \quad (1.6)$$

and

$$|\mathbf{E}_0(R, 0, \theta)| = \frac{|B_1(\theta)|}{R} \quad (1.7)$$

A study of (1.6) and Figure 1.1 will reveal that $|B_1(\theta)|/R$ is the H-plane amplitude pattern measured as a function of θ at a distance R from the origin. The term $\Phi_{B_1}(\theta)$ in (1.6) is the H-plane phase pattern. If $\phi = \pi/2$, (1.5) becomes

$$\mathbf{E}_0(R, \pi/2, \theta) = \frac{|A_1(\theta)|}{R} e^{-j[\kappa R - \Phi_{A_1}(\theta)]} \mathbf{a}_\theta \quad (1.8)$$

Then

$$|\mathbf{E}_0(R, \pi/2, \theta)| = \frac{|A_1(\theta)|}{R} \quad (1.9)$$